European Journal of Echocardiography (2008) **9**, 225–234
doi:10.1016/j.euje.2007.04.002

Echocardiography in the assessment of right heart function

Per Lindqvist[1,3]*, Avin Calcutteea[2] and Michael Henein[2,3]

[1]*Departments of Clinical Physiology,* [2]*Cardiology Heart Centre; and* [3]*Public Health and Clinical Medicine, Umeå University, Umeå University Hospital, Sweden*

Received 5 December 2006; accepted for revision 28 April 2007; online publish-ahead-of-print 25 June 2007

KEYWORDS
Right ventricle;
Doppler tissue imaging;
Strain echocardiography;
Speckle tracking echocardiography

Assessment of right heart function remains difficult despite rapid technological echocardiographic developments. This review addresses the anatomical and physiological basis for assessment of right ventricular function. It also addresses advantages and limitations of individual echocardiographic techniques currently used in clinical and academic practice. The review concludes that volume calculation and estimation of ejection fraction is not ideal for clinical assessment of right ventricular function. Regional myocardial wall motion detection by M-mode and tissue Doppler velocities are probably the best useful methods in clinical practice. 1D and 2D strain, velocity vector imaging and 4D echocardiography need further evaluation before considering them as routine investigations. A global interest needs to be given to a very important neglected entity, 'right ventricle', which has been shown to predict exercise tolerance and outcome in a number of syndromes.

Introduction

Normal anatomy and physiology

The right ventricle (RV) is anatomically placed beneath the sternum and anteriorly positioned to the left ventricle (LV). RV muscle mass is approximately one-sixth that of the LV explained by different loading conditions, as it pumps against approximately one-sixth the resistance of the LV. While the LV, under normal conditions, is thick walled and ellipsoid in shape, the RV is thin walled (3–4 mm) and crescent shaped.[1] Furthermore, the RV is anatomically, structurally and functionally divided into two parts, the inflow (IT) and outflow tract (OT) (*Figure 1*) separated by a thick intracavitary muscle band, the crista supraventricularis.[2] A second intracavitary muscle, the moderator band which is attached to the RVOT,[3] runs from the septum to the anterior RV wall. The apical part of the RV is heavily trabeculated and virtually an immobile part of the ventricle.

The IT is mainly composed of circumferential fibres in the subepicardium and longitudinal fibres in the subendocardium. At the OT, both subendocardial and subepicardial fibres run longitudinally, overlaid by fibres running at right angle to the outlet long axis in a circumferential fashion, which can be traced to the crista supraventricularis and to the anterior ventricular sulcus, serving to bind the two ventricles together.[4] The muscular architecture of the outflow tract is described as a bulbar musculature, which is anatomically and functionally different from the rest of the RV[3,5]. However, the functional role of the RVOT is still not fully understood[6] but believed to serve as a guard to the pulmonary circulation during pressure rise in the RV.[5,7] The thin-walled RV ejects the same rate and volume of blood as the thick-walled LV and this can be explained by studying the characteristics of the pulmonary circulation compared to the systemic circulation.[8]

The RV wall motion is complex.[9,10] During systole, at the IT there is a longitudinal shortening from base to apex and a radial motion towards the common septum. Additional circumferential motion gives a rotation or a squeeze of the ventricle.[11] During the phase of isovolumic contraction the ventricle moves in a circumferential direction controlled by the subepicardial fibres. The longitudinal shortening of the RV occurs mainly during the ejection phase of the cardiac cycle controlled by the subendocardial fibres. The onset of the RV ejection at OT occurs approximately 25 ms after the contraction of the IT which gives an overall peristaltic ventricular motion.[5] The contribution of the septal motion to RV function in the normal heart and in different disease states is not fully understood, but is considered to contribute to both the LV and RV function[12,13] and is a major determinant of overall RV performance.[14]

* Corresponding author. Tel: +46 90 785 1965; fax: +46 90 137633.
E-mail address: per.lindqvist@medicin.umu.se (P. Lindqvist).

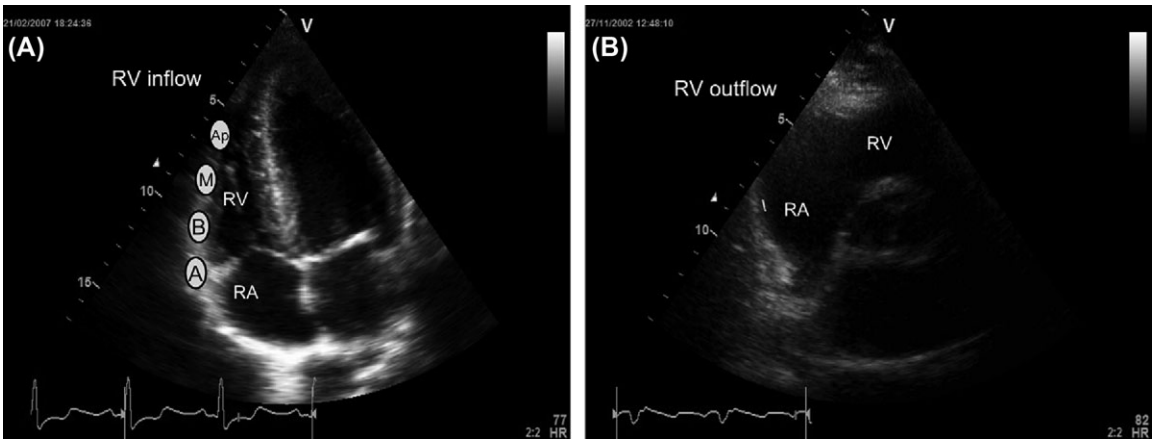

Figure 1 Echocardiographic views of the right ventricle (RV). (*A*) The RV viewed from apical four-chamber view with the right atrium (RA) and the inflow tract of the RV. (*B*) The RV is viewed from parasternal short axis view with RV outflow tract visualized. A, annular level; B, basal level; M, mid level; Ap, apical level.

Abnormal anatomy and physiology

The thin wall of the RV makes it sensitive to alterations in the pulmonary artery pressure. In a normal heart, the RV usually ejects against a low impedance circulation, compared to the left ventricle. With chronic increase in afterload, the RV dilates and develops muscular hypertrophy. The change in RV size, due to pressure or volume overload, may affect the cardiac output. With rapid increase in afterload (i.e. pulmonary artery pressures) e.g. in acute pulmonary embolism, the RV enlarges causing dilatation of the tricuspid annulus and hence tricuspid regurgitation. If this is not promptly treated, alterations of intrinsic myocardial characteristics occur and RV end diastolic and right atrial (RA) pressures rise and hence the clinical signs of right ventricular failure with its known poor outcome.[15]

As is the case with the left ventricle, maintaining coronary flow to the RV is crucial, especially when RV systolic pressure is elevated. In pulmonary hypertension, RV myocardial oxygen demand is increased and right coronary artery (RCA) perfusion pressure may be unchanged or decreased. Since RV perfusion occurs during both diastole and systole, the systolic component is reduced as a result of the raised chamber pressures.[16,17] The RV is involved in approximately 40–50% of patients with acute inferior infarction and may result in a haemodynamic compromised situation with a poor clinical outcome.

In most patients with multi-vessel coronary artery disease the RV demonstrates significant long axis motion dysfunction with stress which affects cardiac output. The RV often becomes volume dependent and patients with RV infarction commonly respond favourably to volume treatment and early reperfusion enhances recovery of RV performance and improves clinical outcome.[18]

Pulmonary diseases affect RV function as a result of elevated pulmonary artery pressures and resistance. Chronic obstructive pulmonary disease (COPD) results in a wide range of resting pulmonary artery pressures and different grades of RV dysfunction.[19–21] During exercise, RV function may further deteriorate in patients with COPD[22] in response to the increased oxygen demand. Studies have shown a fall in long axis function in patients with cystic fibrosis[23] and diastolic dysfunction in patients with COPD and pulmonary embolism.[24]

Prognostic studies have shown RV function as a major determinant of symptoms and exercise capacity in heart failure[25] with poor outcome in patients with depressed RV long axis function, right atrial dilatation and vena cava dilatation.[26–28] A consistent rise in pulmonary pressures, secondary to long-standing severe mitral or aortic valve disease, commonly affects the RV ejection fraction. As a matter of fact, the tricuspid annulus might also dilate causing severe tricuspid regurgitation which may lead to severe right heart failure. However, successful management of the underlying pathology may improve RV function. Mitral valve diseases directly influence the pulmonary pressures and RV function more than aortic valve diseases. However, once irreversible pulmonary vascular disease develops, PA pressures may remain elevated even after a successful valve or myocardial surgery.[29,30] Therefore, early detection of pulmonary hypertension (PHT) is important in optimizing patient management.

Finally, a reduced RV long axis motion is a common finding after open heart surgery.[31] The reason for this is not fully understood. Pericardiectomy with loss of lubricating surface at the anterior surface of the heart, ischaemic damage due to non-optimal RV myocardial preservation during cardiac surgery, and right atrial damage due to placement of bypass cannulae have all been proposed as possible explanations.[32]

Ventricular interaction

The right and left ventricles are closely related because of the anatomical basis of their morphology. The two ventricles share the inter-ventricular septum which mostly functions as part of the left ventricle in normal hearts. With right-sided volume or pressure overload, the interventricular septal motion is reversed and the septum functions as part of the right ventricle (*Figure 2A,B*). After bypass circulation and a fall in RV free wall function, irrespective of the procedure used, septal movement reverses and becomes right ventricular, probably for the same reason of maintaining RV stroke volume (*Figure 2C*). The septum also transmits pressures between the two cavities. Patients with raised LV end-diastolic pressure may present with a dominant 'a' wave in the jugular venous

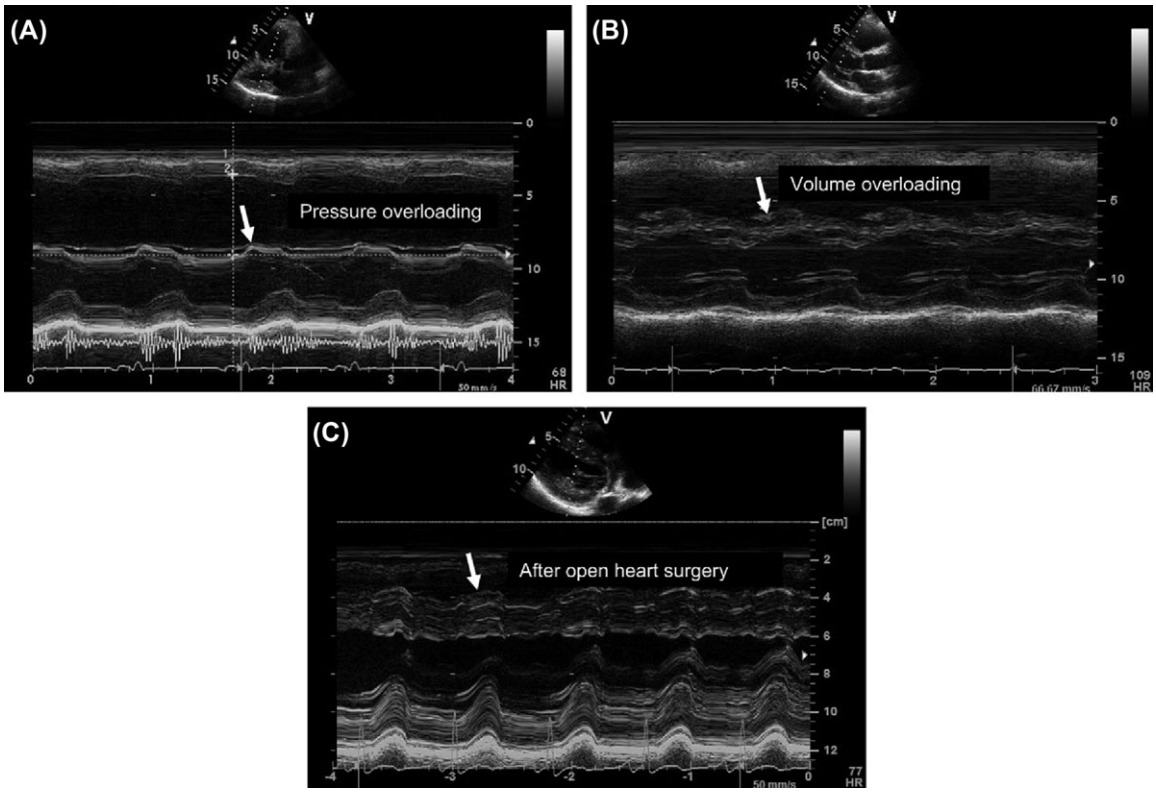

Figure 2 Different interventricular septal wall motion abnormalities due to: (*A*) pressure overloading, arrow showing systolic septal shift; (*B*) volume overloading, arrow showing diastolic septal shift; (*C*) after open heart surgery, arrow showing systolic septal shift.

pulse that reflects left-sided end-diastolic pressures. The same principle applies in patients with pericardial constriction who present with pressure equalization between the two chambers. Finally, in patients with restrictive LV physiology the raised left-sided atrio-ventricular pressure gradient in early diastole is transmitted to the right side which results in suppressed early diastolic right ventricular filling. These disturbances have been shown to reverse with successful off loading of the left atrium and normalization of left-sided pressures.[33] The right and left ventricles are also linked due to the fact that they are both enclosed within the pericardium. Although changes in intra-pericardial pressure, irrespective of their aetiology affect primarily the right heart, the left heart may also be affected if the right-sided problem is not promptly managed. Increased intrapericardial pressure, due to rapid accumulation of pericardial effusion results in phasic filling and ejection of the right ventricle with respiration, being predominant during inspiration. This, if ignored, may result in reciprocal left-sided behaviour during expiration. Similar disturbed physiology could be seen with large pleural effusion and even with end-stage pulmonary disease.[34]

Echocardiography in the assessment of right heart function

M-mode echocardiography

Two-dimensional guided M-mode measurements of systolic long axis motion of the RV free wall is an attractive tool due to its simplicity[35,36] and has been shown to correlate with ejection fraction derived by radionuclide angiography.[27] It has also been shown to be valuable in assessing ischaemic heart disease and cardiomyopathy.[33] The main limitation in assessing RV function using the long axis motion is that it only represents the inflow free wall segments, thus missing the outflow tract and the septal contribution to the overall function of the RV. Additional measurements of RV outflow tract fractional shortening add great value. This method has been found to correlate better with pulmonary artery systolic pressure compared to long axis motion.[37] Finally, RV end-diastolic diameter from the parasternal projection can easily be used as a measurement of dimension (*Table 1*).[38] *Figure 3* shows the echocardiographic assessment of right ventricular outflow tract normal fractional shortening (*Figure 3A*) (RVOTfs) measured by M-mode and the RV normal long axis motion or tricuspid annular plane systolic excursion (*Figure 3B*) (TAPSE). Note that end-diastolic measurements are taken at the onset of the q-wave and end-systolic measurements at the end of the T-wave or pulmonary component of the second heart sound of the phonocardiogram, if available.

Two-dimensional echocardiography

Two-dimensional (2D) echocardiography (*Table 2*) is today a well-established cardiac investigation worldwide. However, as the RV is positioned close to the sternum and also being complex in its geometrical shape, assessment by 2D echocardiography may be limited. Volume and ejection fraction calculations using Simpson's formula are based on mathematical assumptions of RV geometry, therefore subject to inaccuracies and not useful in clinical practice. RV end-diastolic and end-systolic areas and the calculated fractional

Table 1 Normal values for M-mode echocardiography measurements of the right ventricle

	Mean ± SD	*N*	Age (years)	Male/Female	Reference
RVEDD, mm	24.3 ± 6.7	36	61 ± 10	21/15	Lindqvist *et al.*[38]
RVOTt, mm	3.3 ± 1.0	36	61 ± 10	21/15	Lindqvist *et al.*[38]
RVOT fs, %	65 ± 14	36	61 ± 10	21/15	Lindqvist *et al.*[38]
TAPSE, mm	25.5 ± 4.7	36	61 ± 10	21/15	Lindqvist *et al.*[38]

EDD, end-diastolic diameter; OTt, outflow tract thickness; fs, fractional shortening; TAPSE, tricuspid annular plane systolic excursion.

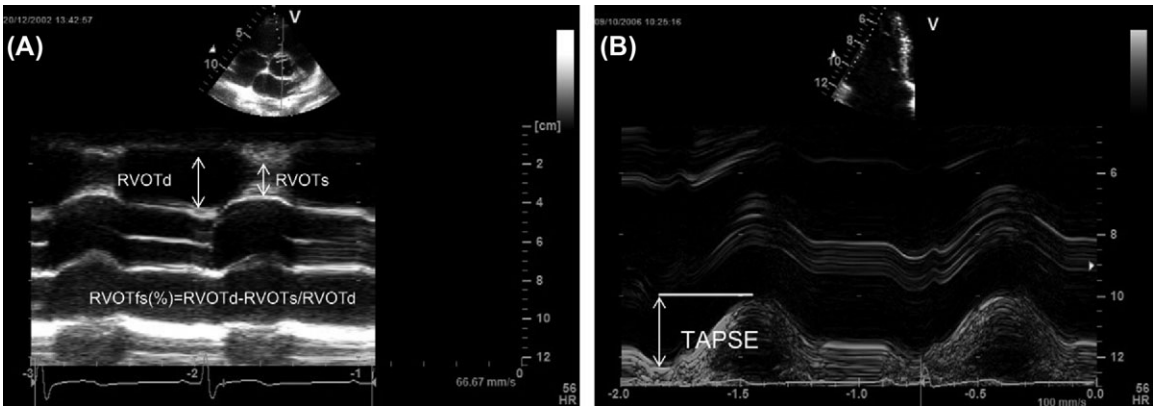

Figure 3 Measurements of (*A*) RVOT fractional shortening (fs%) and (*B*) tricuspid annular plane excursion (TAPSE). S, systole; D, diastole.

Table 2 Normal values for 2D echocardiography measurements of the right atrium and ventricle

	Mean ± SD	*N*	Age (years)	Male/Female	Reference
RA area, cm^2	13 ± 2	25	56 ± 16	4/21	Lindqvist *et al.*[44]
RV wall thickness, mm	4.0 ± 0.7	41	32(19–46)	20/21	Foale *et al.*[1]
RVED inflow area, cm^2	17 ± 3	30	52 ± 20	15/15	Lopez-Candales *et al.*[45]
RVES inflow area, cm^2	8 ± 3	30	52 ± 20	15/15	Lopez-Candales *et al.*[45]
RV inflow FAC, %	51 ± 11	30	52 ± 20	15/15	Lopez-Candales *et al.*[45]
RVEF, % (Simpson)	46 ± 7	100	59 ± 16	49/51	Hsiao *et al.*[46]
RVED outflow diameter, mm	27 ± 2	41	32(19–46)	20/21	Foale *et al.*[1]

RA, right atrial; ED, end diastolic; ES, end systolic; FAC, fractional area change; EF, ejection fraction.

area change including the trabeculated apical part, reflect global and regional wall motion and can be measured both manually and with automatic edge detection.[39–41] The McConnell sign, i.e. basal and mid segmental RV hypokinesia with preserved apical wall motion, has been reported in patients with pulmonary embolism and those with RV infarction.[42] Finally, right atrial area can easily be measured from the apical four-chamber view. From the subcostal view, evaluation of pericardial effusion and its involvement with RV free wall function can be achieved. Additional estimation of right atrial pressure can be obtained from measuring the inferior vena cava dimensions and its diameter variation during normal breathing or sniff test. A reduction in inferior vena cava (IVC) diameter of more than 50% is consistent with right atrial pressure <10 mmHg.[43]

Conventional Doppler echocardiography

Continuous wave Doppler is used to estimate pulmonary artery systolic and mean diastolic pressure by measuring the peak retrograde pressure drop across the tricuspid valve (TR) and pulmonary valve (PR), respectively (*Table 3*). Tricuspid valve velocities can be obtained from parasternal short or long axis projection and apical view whereas pulmonary valve velocities are obtained from the parasternal short axis views (*Figure 1B*). The pressure drop (gradient) is calculated from the flow velocity using the modified Bernoulli formula ($\Delta P = 4V^2$). The hepatic venous flow can also be used for estimating right atrial pressure, and consequently calculating pulmonary artery systolic and mean diastolic pressures.[47] Pulsed Doppler recordings of pulmonary valve flow acceleration time (PAat), pre-ejection period (PEP) and ejection time (PAet) at the RV outflow tract and the RV isovolumic relaxation time (IVRt) from trans-tricuspid flow may also be used to estimate pulmonary artery pressure and resistance.[48,49] Peak TR gradient is today the most commonly used method to assess pulmonary artery systolic pressure in clinical practice.[50]

A new method, the Tei or myocardial performance index (MPI), is used to assess overall RV function. It is calculated

Table 3 Normal values for Doppler echocardiography measurements of the right ventricle

	Mean ± SD	*N*	Age (years)	Male/Female	Reference
PAat, ms	141 ± 29	25	56 ± 16	21/4	Lindqvist *et al.*[44]
PAPEP, ms	91 ± 18	25	56 ± 16	21/4	Lindqvist *et al.*[44]
PAet, ms	310 ± 39	25	56 ± 16	21/4	Lindqvist *et al.*[44]
TF E, cms	43 ± 11	255	58 ± 19	130/125	Lindqvist *et al.*[55]
TF A, cm/s	31 ± 10	255	58 ± 19	130/125	Lindqvist *et al.*[55]
TF E/A	1.5 ± 0.8	255	58 ± 19	130/125	Lindqvist *et al.*[55]
TF IVRT, ms	31 ± 16	255	58 ± 19	130/125	Lindqvist *et al.*[55]
TF IVRT/RR, %	4.2 ± 1.7	25	56 ± 16	21/4	Lindqvist *et al.*[55]
TFDT, ms	187 ± 58	255	58 ± 19	130/125	Lindqvist *et al.*[55]
RV MPI	0.28 ± 0.04	70	50 ± 17	–	Eidem *et al.*[52]
RA-RVgrad, mm Hg	22 ± 6	255	58 ± 19	130/125	Lindqvist *et al.*[55]
HVFs, cm/s	0.42 ± 0.08	10	28.7	–	Hammarstrom *et al.*[56]
HVFd, cm/s	0.23 ± 0.11	10	28.7	–	Hammarstrom *et al.*[56]

PA, pulmonary artery; at, acceleration time; pep, pre-ejection period; et, ejection time; TF, tricuspid flow; E, early diastolic; A, late atrial; IVRT, isovolumic relaxation time; RR, R-R time interval; DT, deceleration time; MPI, myocardial performance index; HVF, hepatic venous flow; s, systole; d, diastole.

Table 4 Normal values for pulsed DTI myocardial velocities and timings at basal and mid segmental levels of the right ventricular free wall

	Mean ± SD	*N*	Age (years)	Male/Female	Reference
Basal (B)					
IVCm, cm/s	15.1 ± 6.1	255	58 ± 19	130/125	Lindqvist *et al.*[55]
Ejm, cm/s	15.2 ± 2.8	255	58 ± 19	130/125	Lindqvist *et al.*[55]
Em, cm/s	14.5 ± 3.5	255	58 ± 19	130/125	Lindqvist *et al.*[55]
Am, cm/s	16.2 ± 3.1	255	58 ± 19	130/125	Lindqvist *et al.*[55]
IVCt, ms	91 ± 26	255	58 ± 19	130/125	Lindqvist *et al.*[55]
IVRt, ms	53 ± 28	255	58 ± 19	130/125	Lindqvist *et al.*[55]
EJt, ms	263 ± 35	255	58 ± 19	130/125	Lindqvist *et al.*[55]
Mid (M)					
IVCm, cm/s	15.5 ± 6.0	255	58 ± 19	130/125	Lindqvist *et al.*[55]
Ejm, cm/s	14.5 ± 2.6	255	58 ± 19	130/125	Lindqvist *et al.*[55]
Em, cm/s	14.1 ± 3.7	255	58 ± 19	130/125	Lindqvist *et al.*[55]
Am, cm/s	16.6 ± 5.5	255	58 ± 19	130/125	Lindqvist *et al.*[55]
IVCt, ms	100 ± 30	255	58 ± 19	130/125	Lindqvist *et al.*[55]
IVRt, ms	58 ± 38	255	58 ± 19	130/125	Lindqvist *et al.*[55]
EJt, ms	259 ± 38	255	58 ± 19	130/125	Lindqvist *et al.*[55]

v, velocity; t, time; IVC, isovolumic contraction; Ej, ejection; E, early diastolic velocities; A, late diastolic velocities; IVR, isovolumic relaxation.

as the ratio between total RV isovolumic time (contraction and relaxation) divided by pulmonary ejection time. The RV MPI has been found to correlate with pulmonary pressures[51] and can be used to identify early RV dysfunction in different diseases.[52,53] The main limitation of the MPI is with increased right atrial pressure when the MPI falls due to shortened isovolumic relaxation time.[54] Finally, relative pulmonary pre-ejection time to aortic pre-ejection time reflects the degree of ventricular dysfunction.

Myocardial Doppler tissue imaging

Doppler tissue imaging (DTI) is a relatively new echocardiographic tool in the assessment of myocardial function (*Tables 4 and 5*). The method is available in most modern ultrasound systems and can provide accurate information on myocardial motion throughout the cardiac cycle.[57,58] In contrast to traditional pulsed Doppler echocardiography, which detects high velocity with low amplitudes, DTI detects low velocity with high amplitudes. To display tissue velocities, two relatively simple alterations in the Doppler signal are required: (i) the high-pass filter is by-passed and (ii) lower gain amplification is used to eliminate the weaker intensity blood flow signals.[59] Tissue velocities can be displayed with spectral pulsed or colour-encoded Doppler visualized with 2D, M-mode or Doppler signals.[57] DTI is proposed to be less preload dependent compared to the traditional pulsed Doppler technique.[60] Typical recordings display 5 main velocity components and 3 time intervals that can be measured (*Figure 4A,B*). Any evidence of asynchrony appears in the form of wrongly timed segmental movements. Longitudinal RV myocardial velocities are obtained from the apical four-chamber view and tracings are best recorded from the annulus (A), basal (B) and mid (M) segmental levels of the RV free wall (*Figure 1A*, *Table 6*).[61]

Pulsed DTI is simpler and more robust to use, with high temporal resolution.[62] The major disadvantages of pulsed DTI are poor spatial resolution due to movement of the heart, while the sample volume is fixed and apical velocities

Table 5 Normal values for color DTI of the right ventricular free wall at basal and mid segments

	Mean ± SD	*N*	Age (years)	Male/Female	Reference
Basal (B)					
IVCm, cm/s	8.3 ± 3.3	106	64.3 ± 9.5	64/42	Yu *et al.*[65]
Ejm, cm/s	9.7 ± 1.9	106	64.3 ± 9.5	64/42	Yu *et al.*[65]
Em, cm/s	8.6 ± 2.3	106	64.3 ± 9.5	64/42	Yu *et al.*[65]
Am, cm/s	11.5 ± 2.8	106	64.3 ± 9.5	64/42	Yu *et al.*[65]
IVCt, ms	64 ± 16	106	64.3 ± 9,5	64/42	Yu *et al.*[65]
IVRt, ms	22 ± 24	33	68 ± 12	9/24	Dambrauskaite *et al.*[66]
Mid (M)					
IVCm, cm/s	6.1 ± 2.7	106	64.3 ± 9.5	64/42	Yu *et al.*[65]
Ejm, cm/s	7.1 ± 1.8	106	64.3 ± 9.5	64/42	Yu *et al.*[65]
Em, cm/s	7.1 ± 2.4	106	64.3 ± 9.5	64/42	Yu *et al.*[65]
Am, cm/s	8.9 ± 3.3	106	64.3 ± 9.5	64/42	Yu *et al.*[65]
IVCt, ms	63 ± 15	106	64.3 ± 9,5	64/42	Yu *et al.*[65]

v, velocity; t, time; IVC, isovolumic contraction; EJ, ejection; E, early diastolic velocities; A, late diastolic velocities; IVR, isovolumic relaxation.

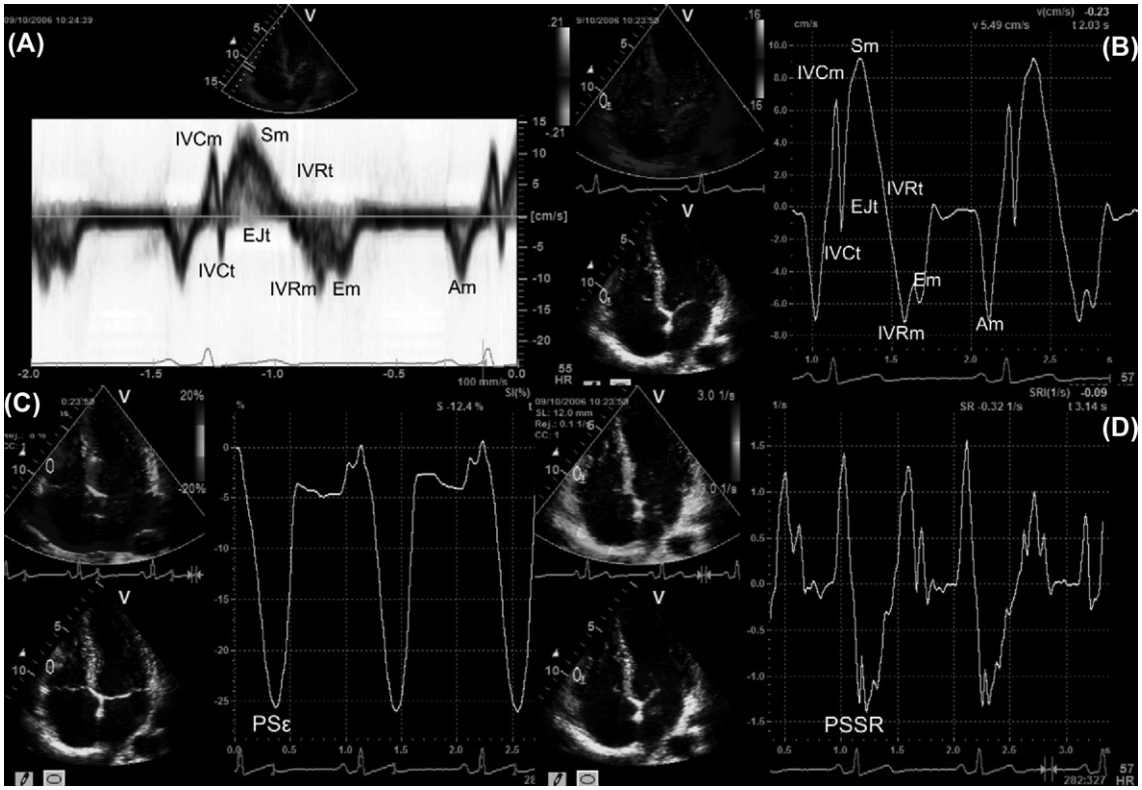

Figure 4 (*A*) Measurements from pulsed Doppler tissue imaging (peak myocardial velocities). IVCm, isovolumic contraction peak positive velocity; IVCt, isovolumic contraction time, defined as time difference between end of A_m to onset of S_m; S_m, systolic (ejection) peak velocity; EJt, ejection time defined as time difference between onset to end of EJt; IVRm, isovolumic relaxation peak negative velocity; IVRt, isovolumic relaxation time, defined as time difference between end of EJt to onset of E_m; E_m, early diastolic peak velocity; A_m, atrial peak velocity. (*B*) Measurements from colour Doppler tissue imaging. For abbreviations see A. (*C*) Strain (ε) echocardiography from a subject with normal systolic RV function at RV free basal level with peak systolic strain (PSε) of −26%. (*D*) Strain rate (SR) echocardiography from a subject with normal systolic RV function at RV free basal level with peak systolic SR (PSSR) of $-1.4\ s^{-1}$.

from the apical long axis projection are difficult to measure.[63] Colour DTI is an alternative approach to measuring myocardial motion and can be used off-line, therefore is favoured for simultaneous wall motion analysis, exercise and stress echocardiography. However, it provides mean values compared to pulsed DTI that provides peak velocities (see *Tables 4* and *5*). The limitation of colour DTI is the lower temporal resolution; however a frame rate above 100 frames per second is considered acceptable.[64] *Figure 4A* demonstrates measurements from pulsed DTI and *Figure 4B* shows the measurements from colour DTI.

One-dimensional strain

Doppler tissue imaging is dependent on the angle at which the region of interest is imaged. Overall heart motion,

Table 6 Normal strain and strain rate values from the right ventricular free wall

	Mean ± SD	*N*	Age (years)	Male/Female	Reference
Basal (B)					
εS, %	−27.7 ± 11.2	36	61 ± 10	15/21	Lindqvist *et al.*[38]
SRs, S^{-1}	−1.5 ± 0.41	40	28.5 ± 5	29/11	Kowalski *et al.*[61]
Mid (M)					
εS, %	−29.4 ± 15.2	36	61 ± 10	15/21	Lindqvist *et al.*[38]
SRs, S^{-1}	−1.72 ± 0.27	40	28.5 ± 5	29/11	Kowalski *et al.*[61]

ε, strain; s, systole; SR, strain rate.

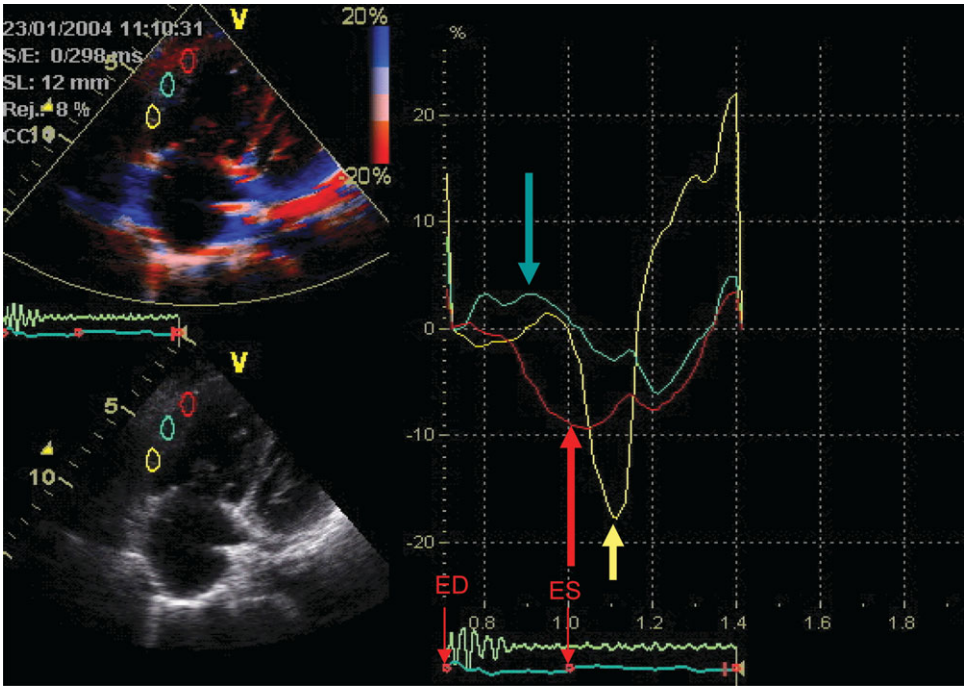

Figure 5 An example of strain echocardiography in pulmonary artery hypertension. Note lengthening during systole at mid segment (blue arrow), delayed peak systolic strain at basal segment (yellow arrow) and best preserved strain at apical segment (red arrow). The tracing example is taken from one cardiac cycle. ED, end diastole; ES, end systole (see colour version of this figure online).

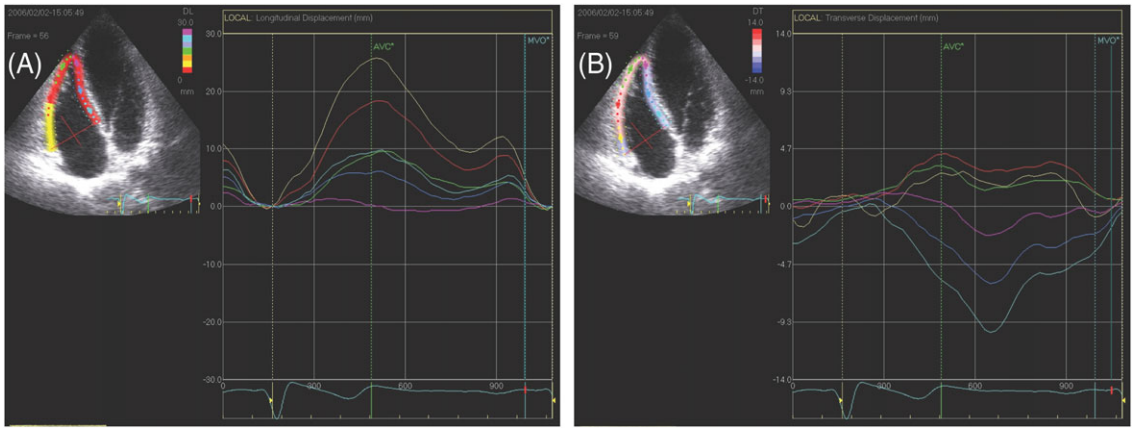

Figure 6 Speckle tracking imaging from the normal right ventricular free wall and septal motion. (*A*) Longitudinal displacement of the right ventricle with the highest amplitude at basal level (yellow segment) compared mid (red) and apical (green). Septal longitudinal motion indicated by light, dark blue and purple color signals. (*B*) Radial displacement towards the cavity of the right ventricle (yellow, green and red) with the highest amplitude at mid segmental level (red segment) and septal radial motion towards the cavity of left ventricle (light blue, dark blue and purple). Tracing examples from one cardiac cycle. AVC, aortic valve closure (see colour version of this figure online).

cardiac rotation and wall motion from tethering segments limit the use of DTI. One-dimensional strain echocardiography is a dimensionless measurement which represents the fractional or percentage change in myocardial fibre shortening. As this myocardial deformation or strain is caused by fibre shortening, it can be used as a measure of 'true' segmental systolic performance.[67]

Strain echocardiography might have a potential input in quantifying regional function in terms of regional myocardial shortening and lengthening. However, how these advantages overcome the disadvantages of signal to noise ratio and angle dependence are still not thoroughly evaluated, thus limiting its clinical routine application. Nevertheless strain and strain rate have shown significant RV abnormalities in patients with amyloidosis,[38] pulmonary hypertension,[68] pulmonary stenosis, atrial septum defects and arrhythmogenic RV dysplasia.[67] Strain measurements of the RV are best performed from the apical four-chamber view, assessing the RV free wall from the base to the apical level. *Figure 4C* and *D* show strain and strain rate echocardiography from a normal RV, and *Figure 5* illustrates an example of strain in pulmonary hypertension.

Two-dimensional strain and velocity vector imaging

The latest of image acquisitions is based on detecting speckles from the myocardium with 2D echocardiography analysing motion in different directions, longitudinal, radial and circumferential.[68–70] This is mainly used for studying the left and right ventricular function but also in the thin-walled right ventricle.[71,72] More studies are needed to evaluate the use of this technique in RV function in great detail. *Figure 6* shows 2D strain speckle tracking from the normal right ventricle.

Three- and four-dimensional echocardiography

Three- and four-dimensional (3/4D) echocardiography may have a potential advantage in determining RV volumes and image reconstruction can be performed both off-line and on-line.[73–75] Today, new solutions for real-time acquisitions are available but the use of this technique remains limited because of the poor lateral resolution in right ventricular cavity dilatation.

Summary

Accurate assessment of right ventricular function remains limited despite rapid technical echocardiographic developments. Volume calculation and estimation of RV ejection fraction is not the method of choice since it is time consuming and limited to the inflow part. Myocardial wall motion measurements and transvalvular velocities, at the inflow and outflow tract by M-mode, conventional Doppler and tissue Doppler velocities are probably the best objective and reproducible methods in clinical practice. Hope remains in the use of 1D and 2D strain, strain rate and 3/4D echocardiography in optimizing accurate measurements of RV function. Since RV function has been shown to be a sensitive predictor of exercise tolerance and outcome in a number of cardiac syndromes, identifying the most sensitive functional markers of RV dysfunction is of immense importance in daily clinical practice.

Acknowledgement

We acknowledge Dr Stellan Mörner for helpful contribution in the preparation of the manuscript.

References

1. Foale R, Nihoyannopoulos P, McKenna W, Kleinebenne A, Nadazdin A, Rowland E et al. Echocardiographic measurement of the normal adult right ventricle. *Br Heart J* 1986;**56**:33–44.
2. Dell'Italia LJ. The right ventricle: anatomy, physiology, and clinical importance. *Curr Probl Cardiol* 1991;**16**:653–720.
3. Grant RP, Downey FM, MacMahon H. The architecture of the right ventricular outflow tract in the normal human heart and in the presence of ventricular septal defects. *Circulation* 1961;**24**:223–35.
4. Greenbaum RA, Ho SY, Gibson DG, Becker AE, Anderson RH. Left ventricular fibre architecture in man. *Br Heart J* 1981;**45**:248–63.
5. Armour JA, Randall WC. Structural basis for cardiac function. *Am J Physiol* 1970;**218**:1517–23.
6. Gibson D. The right ventricular infundibulum: has it a role? *Eur J Echocardiogr* 2003;**4**:3.
7. Keith A. Fate of the bulbus cordis in the human heart. *Lancet* 1924;**ii**: 1267–73.
8. Dell'Italia LJ, Santamore WP. Can indices of left ventricular function be applied to the right ventricle? *Prog Cardiovasc Dis* 1998;**40**:309–24.
9. Rushmer RF, Thal N. The mechanism of ventricular contraction: a cinefluorographic study. *Circulation* 1951;**4**:219–28.
10. Torrent-Guasp F, Buckberg GD, Clemente C, Cox JL, Coghlan HC, Gharib M. The structure and function of the helical heart and its buttress wrapping. I. The normal macroscopic structure of the heart. *Semin Thorac Cardiovasc Surg* 2001;**13**:301–19.
11. Buckberg GD, Coghlan HC, Hoffman JI, Torrent-Guasp F. The structure and function of the helical heart and its buttress wrapping. VII. Critical importance of septum for right ventricular function. *Semin Thorac Cardiovasc Surg* 2001;**13**:402–16.
12. Kaul S. The interventricular septum in health and disease. *Am Heart J* 1986;**112**:568–81.
13. Lindqvist P, Morner S, Karp K, Waldenstrom A. New aspects of septal function by using 1-dimensional strain and strain rate imaging. *J Am Soc Echocardiogr* 2006;**19**:1345–9.
14. Klima U, Guerrero JL, Vlahakes GJ. Contribution of the interventricular septum to maximal right ventricular function. *Eur J Cardiothorac Surg* 1998;**14**:250–5.
15. Ribeiro A, Lindmarker P, Juhlin-Dannfelt A, Johnsson H, Jorfeldt L. Echocardiography Doppler in pulmonary embolism: right ventricular dysfunction as a predictor of mortality rate. *Am Heart J* 1997;**134**:479–87.
16. Ribeiro A, Lindmarker P, Johnsson H, Juhlin-Dannfelt A, Jorfeldt L. Pulmonary embolism: a follow-up study of the relation between the degree of right ventricle overload and the extent of perfusion defects. *J Intern Med* 1999;**245**:601–10.
17. Gomez A, Bialostozky D, Zajarias A, Santos E, Palomar A, Martinez ML et al. Right ventricular ischemia in patients with primary pulmonary hypertension. *J Am Coll Cardiol* 2001;**38**:1137–42.
18. Goldstein JA. Right heart ischemia: pathophysiology, natural history, and clinical management. *Prog Cardiovasc Dis* 1998;**40**:325–41.
19. Matthay RA, Berger HJ. Noninvasive assessment of right and left ventricular function in acute and chronic respiratory failure. *Crit Care Med* 1983;**11**:329–38.
20. Brent BN, Mahler D, Berger HJ, Matthay RA, Pytlik L, Zaret BL. Augmentation of right ventricular performance in chronic obstructive pulmonary disease by terbutaline: a combined radionuclide and hemodynamic study. *Am J Cardiol* 1982;**50**:313–9.
21. Brent BN, Berger HJ, Matthay RA, Mahler D, Pytlik L, Zaret BL. Physiologic correlates of right ventricular ejection fraction in chronic obstructive pulmonary disease: a combined radionuclide and hemodynamic study. *Am J Cardiol* 1982;**50**:255–62.
22. Mahler DA, Brent BN, Loke J, Zaret BL, Matthay RA. Right ventricular performance and central circulatory hemodynamics during upright exercise in patients with chronic obstructive pulmonary disease. *Am Rev Respir Dis* 1984;**130**:722–9.
23. Florea VG, Florea ND, Sharma R, Coats AJ, Gibson DG, Hodson ME et al. Right ventricular dysfunction in adult severe cystic fibrosis. *Chest* 2000; **118**:1063–8.
24. Nakamura K, Miyahara Y, Ikeda S, Naito T. Assessment of right ventricular diastolic function by pulsed Doppler echocardiography in chronic

pulmonary disease and pulmonary thromboembolism. *Respiration* 1995; **62**:237–43.
25. Baker BJ, Wilen MM, Boyd CM, Dinh H, Franciosa JA. Relation of right ventricular ejection fraction to exercise capacity in chronic left ventricular failure. *Am J Cardiol* 1984;**54**:596–9.
26. Mendes LA, Dec GW, Picard MH, Palacios IF, Newell J, Davidoff R. Right ventricular dysfunction: an independent predictor of adverse outcome in patients with myocarditis. *Am Heart J* 1994;**128**:301–7.
27. Ghio S, Gavazzi A, Campana C, Inserra C, Klersy C, Sebastiani R et al. Independent and additive prognostic value of right ventricular systolic function and pulmonary artery pressure in patients with chronic heart failure. *J Am Coll Cardiol* 2001;**37**:183–8.
28. Nath J, Vacek JL, Heidenreich PA. A dilated inferior vena cava is a marker of poor survival. *Am Heart J* 2006;**151**:730–5.
29. Nagel E, Stuber M, Hess OM. Importance of the right ventricle in valvular heart disease. *Eur Heart J* 1996;**17**:829–36.
30. Cohen M, Fuster V. What do we gain from the analysis of right ventricular function? *J Am Coll Cardiol* 1984;**3**:1082–4.
31. Wranne B, Pinto FJ, Hammarstrom E, St Goar FG, Puryear J, Popp RL. Abnormal right heart filling after cardiac surgery: time course and mechanisms. *Br Heart J* 1991;**66**:435–42.
32. Carr-White GS, Kon M, Koh TW, Glennan S, Ferdinand FD, De Souza AC et al. Right ventricular function after pulmonary autograft replacement of the aortic valve. *Circulation* 1999;**100**(19 Suppl):II36–41.
33. Henein MY, O'Sullivan CA, Coats AJ, Gibson DG. Angiotens in converting enzyme (ACE) inhibitors revert abnormal right ventricular filling in patients with restrictive left ventricular disease. *J Am Coll Cardiol* 1998;**32**:1187–93.
34. Henein M, Sheppard M, Pepper J, Rigby M. *Clinical echocardiography.* London: Springer; pp.195–209.
35. Hoffmann R, Hanrath P. Tricuspid annular velocity measurement. Simple and accurate solution for a delicate problem? *Eur Heart J* 2001;**22**:280–2.
36. Kaul S, Tei C, Hopkins JM, Shah PM. Assessment of right ventricular function using two-dimensional echocardiography. *Am Heart J* 1984;**107**: 526–31.
37. Lindqvist P, Henein M, Kazzam E. Right ventricular outflow tract fractional shortening: an applicable measure of right ventricular systolic function. *Eur J Echocardiogr* 2003;**4**:29–35.
38. Lindqvist P, Olofsson BO, Backman C, Suhr O, Waldenstrom A. Pulsed tissue Doppler and strain imaging discloses early signs of infiltrative cardiac disease: a study on patients with familial amyloidotic polyneuropathy. *Eur J Echocardiogr* 2006;**7**:22–30.
39. Forni G, Pozzoli M, Cannizzaro G, Traversi E, Calsamiglia G, Rossi D et al. Assessment of right ventricular function in patients with congestive heart failure by echocardiographic automated boundary detection. *Am J Cardiol* 1996;**78**:1317–21.
40. Geva T, Powell AJ, Crawford EC, Chung T, Colan SD. Evaluation of regional differences in right ventricular systolic function by acoustic quantification echocardiography and cine magnetic resonance imaging. *Circulation* 1998;**98**:339–45.
41. Vignon P, Weinert L, Mor-Avi V, Spencer KT, Bednarz J, Lang RM. Quantitative assessment of regional right ventricular function with color kinesis. *Am J Respir Crit Care Med* 1999;**159**:1949–59.
42. Casazza F, Bongarzoni A, Capozi A, Agostoni O. Regional right ventricular dysfunction in acute pulmonary embolism and right ventricular infarction. *Eur J Echocardiogr* 2005;**6**:11–4.
43. Kircher BJ, Himelman RB, Schiller NB. Noninvasive estimation of right atrial pressure from the inspiratory collapse of the inferior vena cava. *Am J Cardiol* 1990;**66**:493–6.
44. Lindqvist P, Caidahl K, Neuman-Andersen G, Ozolins C, Rantapaa-Dahlqvist S, Waldenstrom A et al. Disturbed right ventricular diastolic function in patients with systemic sclerosis: a Doppler tissue imaging study. *Chest* 2005;**128**:755–63.
45. Lopez-Candales A, Dohi K, Iliescu A, Peterson RC, Edelman K, Bazaz R. An abnormal right ventricular apical angle is indicative of global right ventricular impairment. *Echocardiography* (Mount Kisco, NY) 2006;**23**:361–8.
46. Hsiao SH, Yang SH, Wang WC, Lee CY, Lin SK, Liu CP. Usefulness of regional myocardial performance index to diagnose pulmonary embolism in patients with echocardiographic signs of pulmonary hypertension. *Am J Cardiol* 2006;**98**:1652–5.
47. Ommen SR, Nishimura RA, Hurrell DG, Klarich KW. Assessment of right atrial pressure with 2-dimensional and Doppler echocardiography: a simultaneous catheterization and echocardiographic study. *Mayo Clin Proc* 2000;**75**:24–9.
48. Dabestani A, Mahan G, Gardin JM, Takenaka K, Burn C, Allfie A et al. Evaluation of pulmonary artery pressure and resistance by pulsed Doppler echocardiography. *Am J Cardiol* 1987;**59**:662–8.
49. Hatle L, Angelsen BA, Tromsdal A. Non-invasive estimation of pulmonary artery systolic pressure with Doppler ultrasound. *Br Heart J* 1981;**45**: 157–65.
50. Chan KL, Currie PJ, Seward JB, Hagler DJ, Mair DD, Tajik AJ. Comparison of three Doppler ultrasound methods in the prediction of pulmonary artery pressure. *J Am Coll Cardiol* 1987;**9**:549–54.
51. Vonk MC, Sander MH, van den Hoogen FH, van Riel PL, Verheugt FW, van Dijk AP. Right ventricle Tei-index: A tool to increase the accuracy of non-invasive detection of pulmonary arterial hypertension in connective tissue diseases. *Eur J Echocardiogr* 2006 July 14 [Epub ahead of print].
52. Eidem BW, Tei C, O'Leary PW, Cetta F, Seward JB. Nongeometric quantitative assessment of right and left ventricular function: myocardial performance index in normal children and patients with Ebstein anomaly. *J Am Soc Echocardiogr* 1998;**11**:849–56.
53. Eidem BW, O'Leary PW, Tei C, Seward JB. Usefulness of the myocardial performance index for assessing right ventricular function in congenital heart disease. *Am J Cardiol* 2000;**86**:654–8.
54. Yoshifuku S, Otsuji Y, Takasaki K, Yuge K, Kisanuki A, Toyonaga K et al. Pseudonormalized Doppler total ejection isovolume (Tei) index in patients with right ventricular acute myocardial infarction. *Am J Cardiol* 2003;**91**:527–31.
55. Lindqvist P, Waldenstrom A, Henein M, Morner S, Kazzam E. Regional and global right ventricular function in healthy individuals aged 20-90 years: a pulsed Doppler tissue imaging study: Umea General Population Heart Study. *Echocardiography* (*Mount Kisco, NY*) 2005;**22**:305–14.
56. Hammarstrom E, Wranne B, Pinto FJ, Puryear J, Popp RL. Tricuspid annular motion. *J Am Soc Echocardiogr* 1991;**4**:131–9.
57. Hatle L, Sutherland GR. Regional myocardial function—a new approach. *Eur Heart J* 2000;**21**:1337–57.
58. Isaaz K, Munoz del Romeral L, Lee E, Schiller NB. Quantitation of the motion of the cardiac base in normal subjects by Doppler echocardiography. *J Am Soc Echocardiogr* 1993;**6**:166–76.
59. Garcia MJ, Thomas JD, Klein AL. New Doppler echocardiographic applications for the study of diastolic function. *J Am Coll Cardiol* 1998;**32**: 865–75.
60. Yalcin F, Kaftan A, Muderrisoglu H, Korkmaz ME, Flachskampf F, Garcia M et al. Is Doppler tissue velocity during early left ventricular filling preload independent? *Heart* 2002;**87**:336–9.
61. Kowalski M, Kukulski T, Jamal F, D'Hooge J, Weidemann F, Rademakers F et al. Can natural strain and strain rate quantify regional myocardial deformation? A study in healthy subjects. *Ultrasound Med Biol* 2001; **27**:1087–97.
62. Marwick TH. Clinical applications of tissue Doppler imaging: a promise fulfilled. *Heart* 2003;**89**:1377–8.
63. Pellerin D, Sharma R, Elliott P, Veyrat C. Tissue Doppler, strain, and strain rate echocardiography for the assessment of left and right systolic ventricular function. *Heart* 2003;**89**(Suppl. 3):iii9–17.
64. Lind B, Nowak J, Dorph J, van der Linden J, Brodin LA. Analysis of temporal requirements for myocardial tissue velocity imaging. *Eur J Echocardiogr* 2002;**3**:214–9.
65. Yu CM, Lin H, Ho PC, Yang H. Assessment of left and right ventricular systolic and diastolic synchronicity in normal subjects by tissue Doppler echocardiography and the effects of age and heart rate. *Echocardiography* (*Mount Kisco, NY*) 2003;20:19–27.
66. Dambrauskaite V, Delcroix M, Claus P, Herbots L, Palecek T, D'Hooge J et al. The evaluation of pulmonary hypertension using right ventricular myocardial isovolumic relaxation time. *J Am Soc Echocardiogr* 2005;**18**: 1113–20.
67. Sutherland GR, Di Salvo G, Claus P, D'Hooge J, Bijnens B. Strain and strain rate imaging: a new clinical approach to quantifying regional myocardial function. *J Am Soc Echocardiogr* 2004;**17**:788–802.
68. Kjaergaard J, Sogaard P, Hassager C. Right ventricular strain in pulmonary embolism by Doppler tissue echocardiography. *J Am Soc Echocardiogr* 2004;**17**:1210–2.
69. Vannan MA, Pedrizzetti G, Li P, Gurudevan S, Houle H, Main J et al. Effect of cardiac resynchronization therapy on longitudinal and circumferential left ventricular mechanics by velocity vector imaging: description and initial clinical application of a novel method using high-frame rate B-mode echocardiographic images. *Echocardiography* (*Mount Kisco, NY*) 2005;**22**:826–30.
70. Helle-Valle T, Crosby J, Edvardsen T, Lyseggen E, Amundsen BH, Smith HJ et al. New noninvasive method for assessment of left ventricular rotation: speckle tracking echocardiography. *Circulation* 2005;**112**:3149–56.

71. Pirat B, McCulloch ML, Zoghbi WA. Evaluation of global and regional right ventricular systolic function in patients with pulmonary hypertension using a novel speckle tracking method. *Am J Cardiol* 2006;**98**:699–704.
72. Borges AC, Knebel F, Eddicks S, Panda A, Schattke S, Witt C et al. Right ventricular function assessed by two-dimensional strain and tissue Doppler echocardiography in patients with pulmonary arterial hypertension and effect of vasodilator therapy. *Am J Cardiol* 2006;**98**:530–4.
73. Papavassiliou DP, Parks WJ, Hopkins KL, Fyfe DA. Threedimensional echocardiographic measurement of right ventricular volume in children with congenital heart disease validated by magnetic resonance imaging. *J Am Soc Echocardiogr* 1998;**11**:770–7.
74. Jiang L, Siu SC, Handschumacher MD, Luis Guererro J, Vazquez de Prada JA, King ME et al. Three-dimensional echocardiography. In vivo validation for right ventricular volume and function. *Circulation* 1994; **89**:2342–50.
75. Kjaergaard J, Sogaard P, Hassager C. Quantitative echocardiographic analysis of the right ventricle in healthy individuals. *J Am Soc Echocardiogr* 2006;**19**:1365–72.